

## The structure of the Kuroshio southwest of Kyushu: velocity, transport and potential vorticity fields

CHANGSHENG CHEN,\* ROBERT C. BEARDSLEY† and RICHARD LIMEBURNER‡

(Received 26 April 1990; in revised form 29 March 1991; accepted 2 April 1991)

**Abstract**—A triangular CTD/ADCP survey was made across the Kuroshio southwest of Kyushu aboard the R. V. *Thompson* during January 1986. Due to relatively poor navigation data, a simple averaging technique has been used to convert the ADCP data taken between CTD station pairs into an average absolute velocity normal to the station pair, with a maximum error varying from about  $\pm 5 \text{ cm s}^{-1}$  to less than  $\pm 0.1 \text{ cm s}^{-1}$  depending on the type of navigation data. The average ADCP velocity at 60 m (or 10 m over the shelf) was then used as the reference velocity to calculate the absolute geostrophic velocity through the sides of the study triangle. The results show that the ADCP velocity shear was in reasonably good agreement with the geostrophic shear of the Kuroshio. The Kuroshio entered the study triangle as a coherent current and then split around a tall seamount into two branches as it left the area. The volume transport of the Kuroshio southwest of Kyushu in January 1986 was  $30.3 \pm 2.0 \text{ Sv}$ , and the advective temperature transport was  $27.6 \pm 1.8 \times 10^{14} \text{ W}$ . These values are similar to those reported for the Gulf Stream in the Florida Strait, and a roughly linear correlation exists between temperature and volume transports in both regions. Mass conservation within the study triangle allowed construction of a streamfunction that showed the presence of cyclonic and anti-cyclonic mesoscale eddies to the north and northwest of the core of the Kuroshio. Potential vorticity estimated from the absolute geostrophic velocity field was conserved along streamlines on potential density surfaces except perhaps near a seamount where curvature vorticity must be considered, and the path of the Kuroshio could be traced by the core of maximum potential vorticity. Finally, the Kuroshio was potentially unstable as it flowed along the continental margin in the Okinawa Trough because the gradient of potential vorticity on potential density surfaces changed sign across the Kuroshio. This helps explain the mesoscale frontal and eddy features observed in the cyclonic side of the Kuroshio in the East China Sea.

### 1. INTRODUCTION

As a major component of the North Pacific general circulation, the Kuroshio is responsible for the large poleward mass and heat transports that are essential to mass conservation and to the global heat balance in the North Pacific Ocean. To better understand the general circulation of the North Pacific, it is thus important to know the structure of the Kuroshio and its quantitative contribution to the meridional mass and heat transports. CHEN *et al.* (submitted) have used CTD data obtained aboard the R.V. *Thompson* and R.V. *Washington* during January and July 1986, respectively, to describe the change from winter to summer in the hydrographic structure of the Kuroshio and adjacent water in the East China Sea. Here we will combine CTD and ADCP data obtained during the January

---

\*MIT/WHOI Joint Program, Woods Hole, MA 02543, U.S.A.

†P.O. Department, WHOI, Woods Hole, MA 02543, U.S.A.

1986 R.V. *Thompson* cruise to estimate the absolute geostrophic velocity structure of the Kuroshio, and use this to describe the mass and temperature transports of the Kuroshio west of Kyushu in January 1986.

The study of transport of the Kuroshio can be traced back to World War II during which most of the observations were made south of Japan by Japanese fishermen and navigators. Since then, many studies have been made on the Kuroshio from its beginning near Luzon Island to the Kuroshio extension at 40°N. However, unlike the Gulf Stream system where absolute volume transports are relatively well known from combined hydrographic and direct current measurements, very few good estimates of the absolute transport of the Kuroshio have yet been made. Most previous estimates have been based on geostrophic calculations that assume a deep reference level of no-motion.

The development of modern direct current measurement techniques has allowed direct determination of the reference level velocity and thus calculation of the absolute geostrophic velocity. JOYCE *et al.* (1982) and REGIER (1982) first applied the shipboard ADCP to make direct current measurements during hydrographic surveys. The methodology for using the ADCP as a survey tool has been developed and described by JOYCE *et al.* (1982, 1986 and 1988) and KOSRO (1985), and this approach has found increasing application in coastal circulation and Gulf Stream studies (KOSRO, 1985; JOYCE *et al.*, 1986; BARTH and BRINK, 1987). BRYDEN *et al.* (1991) were the first to combine CTD and ADCP data to estimate the absolute geostrophic velocity across the Kuroshio southeast of the Ryukyu Islands. They also had collected CTD and ADCP data across the Kuroshio in the Tokara Strait, but decided not to calculate absolute geostrophic velocities due to the poor Loran-C navigation coverage in that region.

We also experienced poor Loran-C reception during the January 1986 R.V. *Thompson* cruise in the East China Sea southwest of Kyushu, so we have developed a simple averaging technique to convert ADCP data into an average absolute velocity normal to the transect between adjacent hydrographic stations. Using this average ADCP velocity as a reference level velocity, we can then calculate the absolute geostrophic velocity and associated fields in the Kuroshio. Since our primary interest here is to describe the structure of the Kuroshio southwest of Kyushu, most of this work will focus on the triangular survey made across the Kuroshio centered near 31°N, 128°E (see Fig. 1). This is an interesting and dynamically important oceanographic region in many respects. First, the Kuroshio enters the Tokara Strait through this region and then increases significantly in its transport south of Japan. Thus, from a dynamical point of view, this region is most similar to the Florida Strait in the Gulf Stream system (NAGATA, 1981). Second, previous theoretical studies suggest that the Kyushu coast is a perturbation source for the bimodality of the Kuroshio south of Japan, so that detailed knowledge of the structure of the Kuroshio in this region may be helpful to understand better the meandering of the Kuroshio (CHAO and McCREARY, 1982). Third, the study region is connected to the wide shelf region of the East China Sea so that the interaction between shelf currents and the Kuroshio may be significant. Finally, the bottom topography west of Kyushu is quite complex and may have a strong influence on the pattern of flow in the Kuroshio.

This paper introduces a simple technique to calculate water velocity from ADCP data in the case where Loran-C navigation coverage is relatively poor. The average water velocity at 60 m (or 10 m over the shelf) between CTD station pairs is then used as the reference level velocity to calculate the absolute geostrophic velocity and transports for all sides of the triangle. The absolute volume and advective temperature transports of the Kuroshio

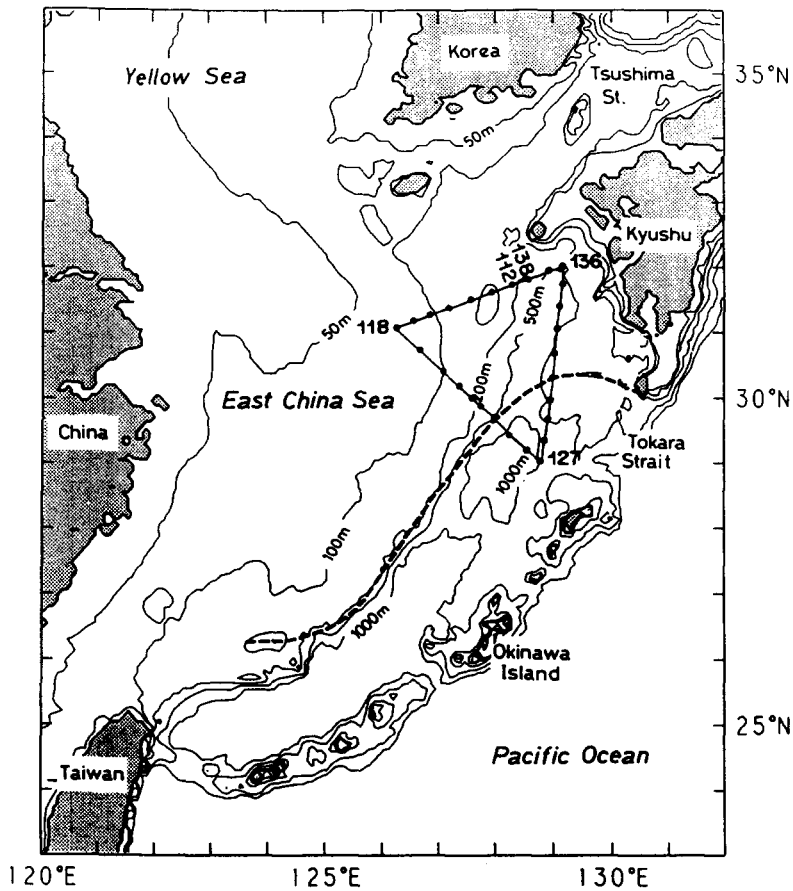


Fig. 1. Map of the East China Sea region, showing the location of the CTD stations made southwest of Kyushu during the R.V. *Thompson* cruise from 28 January to 1 February 1986. The survey was conducted in a counterclockwise sense around the triangle, and the stations are numbered sequentially in time from 112 to 138.

during January 1986 are estimated based on the absolute geostrophic velocity field. Since the volume transport through the triangular domain was conserved within measurement uncertainty, a set of streamlines are defined by the volume transports to describe the horizontal structure of the flow field in the Kuroshio and its adjacent currents. Finally, two potential vorticity sections across the Kuroshio are presented, that illustrate how the path of the Kuroshio can be traced through the study triangle by its core of maximum potential vorticity.

## 2. A TECHNIQUE FOR ADCP DATA TREATMENT

Joyce (1989) has derived expressions for the true water velocity in which the ADCP misalignment and sensitivity errors are defined and calculated. Let the  $(x,y)$  coordinate system be the true east, north coordinate frame in which the position and velocity of the ship are determined, and the  $(x',y')$  frame be that of the ADCP in which the velocity is

decomposed into the east and north components using the ship's gyro. Then, the absolute velocity (taken here as the water velocity) is equal to the vector sum of the detected Doppler velocity  $\vec{U}_d$  and the ship velocity  $\vec{U}_s$ . In the  $(x, y)$  frame, this can be expressed by

$$U_w = U_s + U_d = U_s + (1 + \beta)(U_d \cos \alpha - V_d \sin \alpha), \quad (2.1)$$

$$V_w = V_s + V_d = V_s + (1 + \beta)(V_d \sin \alpha - U_d \cos \alpha), \quad (2.2)$$

where  $\alpha$  is the counter-clockwise misalignment angle of the ADCP transducer and gyro errors, and  $\beta$  is the correction factor due to sensitivity error.

In shallow regions less than 200 m, the ship's velocity over the bottom can be measured directly with a 150 kHz ADCP. In deeper regions, however, the ship's velocity must be determined by using Loran-C or satellite navigation fixes. If  $\alpha$  and  $\beta$  are known, the error of the estimate of absolute velocity is mainly dependent on that of the ship's velocity. In the Gulf Stream, high quality Loran-C fixes are readily available almost every 3 min (R. WELLER, personal communication), so that accurate estimates of the ship's velocity are possible provided that filtering can remove high-frequency noise. However, on the January 1986 R.V. *Thompson* cruise in the Kuroshio, Loran-C fixes were obtained about every 30 min and only three to four Loran-C fixes were recorded with each pair of CTD stations; thus the resulting calculation of the ship's velocity was relatively poor.

A simple technique is described now to calculate the average water velocity normal to the transect given by each pair of CTD stations. Let  $A$  and  $B$  be the position of the ship at two successive CTD stations, and let  $(\vec{p}, \vec{n})$  be directional unit vectors oriented either parallel or normal to the station pair vector  $\vec{AB}$ , respectively. If the water velocity averaged in time over the distance from  $A$  to  $B$  is denoted by

$$\vec{U}_w = \vec{U}_s + \vec{U}_d, \quad (2.3)$$

$$\vec{V}_w = \vec{V}_s + \vec{V}_d, \quad (2.4)$$

then the average water velocity normal to  $\vec{AB}$  is given by

$$\vec{U}_{wn} = \vec{V}_w \cos \theta - \vec{U}_w \sin \theta = \vec{U}_{sn} + \vec{U}_{dn}, \quad (2.5)$$

where  $\theta$  is the angle between  $\vec{p}$  and  $\vec{x}$ , and  $\vec{U}_{sn}$  and  $\vec{U}_{dn}$  are the normal components of the ship's velocity and ADCP velocity, respectively.

If the ship starts at  $A$  and eventually reaches  $B$ , the average component of the ship's velocity normal to the section  $\vec{AB}$  should vanish (i.e.  $\vec{U}_{sn} = 0$ ), so the average water velocity  $\vec{U}_{wn}$  reduces to

$$\vec{U}_{wn} = \vec{U}_{dn} = -\vec{U}_d \sin \theta + \vec{V}_d \cos \theta. \quad (2.6)$$

On the January 1986 R.V. *Thompson* survey around the study triangle, the bottom velocity was recorded over the shelf from Stas 112–124, and high quality GPS data were recorded from Stas 126–130 and Stas 136–138 (see Fig. 1 for station location). The positions of remaining stations were estimated using Loran-C fixes. Therefore, estimation of absolute velocity should be better on the western section where only three stations were located by Loran-C.

Two main errors must be taken into account when the technique introduced above is applied to find the absolute water velocity from the ADCP data: (1) the bias in the angle  $\theta$  between the station pair orientation  $\vec{AB}$  and the  $x$ -axis of the geographical coordinate

frame, and (2) the misalignment  $\alpha$  and sensitivity  $\beta$  (or ADCP calibration) errors. The error in  $\theta$  results from uncertainty in the ship's position. A simple geometrical analysis reveals that this error is not only dependent on the absolute value of the error circle associated with each position fix but is also inversely proportional to the distance between two stations. The misalignment error  $\alpha$  is caused by the small deviation of the orientation of the transducer head relative to the gyro reference orientation. The sensitivity error  $\beta$  can be caused by errors in the oscillator frequency or speed of sound and spreading of the acoustic beams, etc., which cause the ADCP velocity to be over- or underestimated (see KOSRO, 1985). A detailed estimation of these errors for the January 1986 R.V. *Thompson* ADCP data set has been made by CHEN (1989). After correction, the maximum uncertainty in the average absolute water velocity between CTD station pairs due to ADCP and navigation errors was reduced to about  $\pm 5 \text{ cm s}^{-1}$  (using Loran-C navigation), to  $\pm 1 \text{ cm s}^{-1}$  (using GPS navigation), and to  $< \pm 0.1 \text{ cm s}^{-1}$  (using bottom-tracking) (see Table 1).

It should be pointed out that the averaging technique described above filters out any high resolution spatial and temporal variability in the absolute velocity structure, and does

Table 1. Maximum uncertainty in absolute ADCP velocity normal to CTD station pairs for the January 1986 R.V. *Thompson* survey

Pair	Ship's navigation	ADCP bottom tracking	$\Delta V_{\max}$ ( $\text{cm s}^{-1}$ )
112-113	Loran-C	Yes	$< \pm 0.1$
113-114	GPS	Yes	$< 0.1$
114-115	GPS	Yes	$< 0.1$
115-116	GPS	Yes	$< 0.1$
116-117	Loran-C	Yes	$< 0.1$
117-118	Loran-C	Yes	$< 0.1$
118-119	Loran-C	Yes	$< 0.1$
119-120	GPS	Yes	$< 0.1$
120-121	GPS	Yes	$< 0.1$
121-122	Loran-C	Yes	$< 0.1$
122-123	Loran-C	Yes	$< 0.1$
123-124	Loran-C	Yes	$< 0.1$
124-125	Loran-C	No	$\pm 4.4$
125-125	Loran-C	No	$\pm 3.9$
126-127	GPS	No	$\pm 0.9$
127-128	GPS	No	$\pm 0.7$
128-129	GPS	No	$\pm 0.6$
129-130	Loran-C	No	$\pm 6.4$
130-131	Loran-C	No	$\pm 5.3$
131-132	Loran-C	No	$\pm 5.4$
132-133	Loran-C	No	$\pm 5.6$
133-134	Loran-C	No	$\pm 5.6$
134-135	Loran-C	No	$\pm 5.5$
135-136	Loran-C	No	$\pm 6.2$
136-137	GPS	No	$\pm 0.9$
137-138	GPS	No	$\pm 1.1$
138-139	Loran-C	Yes	$< 0.1$

not allow determination of the two-dimensional current vector field. The average ADCP velocity may still contain some ageostrophic components, such as tidal currents and inertial motions. These have been found to seriously contaminate ADCP data used for geostrophic reference in the open ocean (J. TOOLE, personal communication). However, simple scale analysis (see CHEN, 1989) suggests that ageostrophic motions associated with the barotropic tide and wind-driven inertial oscillations were small in comparison to the strong Kuroshio currents observed during the January 1986 survey.

Using the average normal ADCP velocities at 60 m in the deeper water and 10 m in water shallower than 100 m as reference level velocities, we have calculated the absolute geostrophic velocity through the sides of the study triangle. A linear extrapolation of specific volume anomalies along isobars has been applied to calculate the geostrophic velocity over the slope where a large depth difference occurs between two adjacent CTD stations (GROEN, 1948; REID and MANTYLA, 1976). Based on the absolute geostrophic velocity, we then estimated the volume and advective temperature transports and potential vorticity across each section of the triangle. These results will be discussed next.

### 3. ABSOLUTE GEOSTROPHIC TRANSPORTS

#### *Volume transport*

One problem arising in calculating absolute geostrophic transport is our poor knowledge of the bottom bathymetry along the eastern transect, especially near three seamounts. To overcome this difficulty, we consider two limiting cases. First, we ignore the seamounts completely and assume a smooth deep bottom. Second, we treat the seamounts as rectangular shapes. The true transport should be between these two limits. The total inflow transport of the Kuroshio through the western section of the study triangle in late January 1986 was equal to  $30.3 \pm 2.0$  Sv, while the outflow transports were  $-26.3 \pm 2.7$  Sv through the eastern section and  $-4.6 \pm 0.4$  Sv through the northern section. (In the transport and velocity calculations presented here, we define flow into the study triangle as positive and flow out of the study triangle as negative.) The net transport into the triangle was  $-0.6 \pm 3.3$  Sv. When rectangular seamounts are assumed for the eastern section, the outflow transport on the eastern section increased to  $-30.1 \pm 2.6$  Sv. The real outflow transport on the eastern section was therefore likely between  $-26.3 \pm 2.7$  Sv and  $-30.1 \pm 2.6$  Sv. Considering the size of the experimental uncertainties of these transport estimates, we conclude that total volume transport was conserved in the closed domain formed by the study triangle.

The islands located near the southern corner of the triangle confine the Kuroshio on its southern side, and it is generally believed that the Kuroshio countercurrent is dominant only to the south of these islands (NITANI, 1972). Thus, calculation of transport through the western section of the triangle should include almost all of the transport through the Okinawa Trough. The missed transport due to incomplete coverage can be roughly estimated using the following simple approach. The distance from the southeast corner of the triangle to the nearest island is 10 km. The depth is 800 m at the southeast corner of the triangle and zero at the coast of the island. If the velocity is assumed to be  $60 \text{ cm s}^{-1}$  at the surface and  $10 \text{ cm s}^{-1}$  at the bottom (based on the velocity profile at station pair 125–126), then the mean velocity of  $35 \text{ cm s}^{-1}$  times the cross-sectional area between Sta. 126 and the island yields an estimate of the missed transport of 1.4 Sv, which is only 4.7% of the total

transport. The total transport over the shelf region was almost equal to zero. Since the missed transport is less than the experimental uncertainty of the total transport measured through the western section, we conclude that the measured transport value of  $30.3 \pm 2.0$  Sv represents an accurate estimation of the total Kuroshio transport during late January 1986.

A direct measurement of the Kuroshio current was made south of Kyushu by TAKE-MATSU *et al.* (1986), who used moored current meters to measure the absolute velocity in the upper 1000 m from 1972 to 1982. The total volume transport was estimated to be 25 Sv south of Tanegashima Island at  $30^\circ\text{N}$  and  $131^\circ\text{E}$ , downstream of our study area. In June 1985, Bryden and co-workers made a CTD/ADCP section aboard the R.V. *Thompson* across the Kuroshio southeast of the Ryukyu Islands located near  $26^\circ\text{N}$ ,  $125^\circ\text{E}$ , about 350 km upstream of our study triangle. BRYDEN *et al.* (1991) used Loran-C to remove the ship's velocity from the ADCP data, and then used the resulting ADCP velocity at 100 m as the reference velocity to compute absolute geostrophic velocity and transport. They obtained a volume transport of 26.2 Sv. ICHIKAWA and BEARDSLEY (submitted) have recently used Japanese hydrographic and near-surface GEK data to estimate spatial and temporal variation in Kuroshio volume transport through the East China Sea. While the accuracy of their transport estimates is not as good as those presented here, they find that the Kuroshio transport exhibits a large seasonal variation in the East China Sea, with a maximum transport in late summer that exceeds the minimum transport in early spring by as much as 20 Sv. The absolute geostrophic volume transport estimates of BRYDEN *et al.* (1991) and ours are consistent with this cycle.

The westward outflow transport over the slope region in the western section was about 0.5 Sv (see Fig. 5 for a map of the streamfunction defined by the absolute geostrophic transport; this streamfunction will be discussed in detail in Section 4). This outflow was probably from the main Kuroshio near the western section since there was no evidence of similar T/S properties on the downstream sections. A large countercurrent transport of order 4.1–6.9 Sv was found on the eastern section. At the same time, an outflow transport of 6.8 Sv was seen around the northeastern corner of the triangle from Stas 134 to 137, suggesting that the outflow near the northeastern corner may come from the westward inflow on the eastern section. In addition, on the northern section, an inflow transport of 1.0 Sv was computed for the band of Stas 112–115 and 137–138 as well as 138–112. Based on the results of the T/S analysis presented in CHEN *et al.* (submitted), this inflow may originate partly from the recirculation on the northeast corner of the triangle and partly from the southward flow prevailing around the year over the shelf (NAGATA, 1981).

### Temperature transport

The direct method to calculate heat transport through a section aligned in the  $x$ -direction is given by

$$Q_T = \iint \rho C_p V \theta \, dz dx, \quad (3.1)$$

where  $\rho$  is the fluid density,  $C_p$  the specific heat capacity,  $\theta$  potential temperature and  $V$  the absolute velocity component normal to  $x$ . Since the choice of temperature scale is

arbitrary, the heat transport obtained above is meaningful only when the mass transport through the section vanishes (MONTGOMERY, 1974). For this reason, oceanic heat transport is usually computed on a section across a whole ocean basin based on the assumption that a southward interior mass transport equals the sum of the northward wind-driven Ekman and western boundary current transports. Since our sections only cross the East China Sea, we follow HALL and BRYDEN (1982) instead and consider the temperature transport defined by equation (3.1) with the potential temperature given in degrees centigrade.

The calculation of Kuroshio temperature transport as a part of the total heat transport across the North Pacific Ocean is useful to help understand the contribution of the Kuroshio to the net poleward heat transport. HALL and BRYDEN (1982) calculated the temperature transport of the Gulf Stream in the Florida Strait (the Florida Current) by dividing the velocity and potential temperature into a sum of a barotropic and baroclinic components, i.e.

$$Q_T = \iint \rho C_p \bar{V} \bar{\theta} dz dx + \iint \rho C_p V' \theta C_p dz dx. \quad (3.2)$$

Using the NILER and RICHARDSON (1973) volume transport measurements (where the volume transport equalled 32.9 Sv in summer with an annual average of 29.5 Sv), Hall and Bryden found that the baroclinic temperature transport equalled  $5.0 \times 10^{14}$  W, while the barotropic part was about  $21 \times 10^{14}$  and  $18.8 \times 10^{14}$  W corresponding to the summer and annual volume transports, respectively. Thus, the total temperature transport of the Florida Current was approximately equal to  $23.8 \times 10^{14}$  W for a volume transport of 29.5 Sv and  $26.0 \times 10^{14}$  W for a volume transport of 32.9 Sv. BRYDEN *et al.* (1991) also used the same method to estimate Kuroshio temperature transport, and found that the baroclinic temperature transport at 24°N in June 1985 equalled  $8.9 \times 10^{14}$  W. The associated volume transport of the Kuroshio was estimated to be 26.2 Sv and the mean potential temperature was 11.6°C. If  $C_p = 4.0 \text{ J(g}^\circ\text{C)}^{-1}$  and  $\rho = 1.026 \times 10^6 \text{ g m}^{-3}$ , then the total barotropic temperature transport was  $12.0 \times 10^{14}$  W. Thus, the total temperature transport at 24°N was  $20.9 \times 10^{14}$  W in June 1985. Since the per cent error of the total temperature transport is determined, in general, by the ratio of the velocity error ( $\pm 5 \text{ cm s}^{-1}$  for the ADCP data using Loran-C navigation) to the mean velocity averaged over the section (taken as  $100 \text{ cm s}^{-1}$  in the Kuroshio), we expect the total temperature transport estimated by BRYDEN *et al.* (1991) to have a minimum uncertainty of at least  $\pm 5\%$ . Therefore, the temperature transport of the Kuroshio was  $20.9 \pm 1.1 \times 10^{14}$  W for a volume transport of  $26.2 \pm 1.3$  Sv in June 1985.

In this present work, we consider the study triangle as a closed system. Mass conservation through the triangular domain based on the January 1986 absolute geostrophic velocity calculation allows us to estimate the net heat transport through the study triangle. The total eastward inflow temperature transport on the western section was  $27.6 \pm 1.8 \times 10^{14}$  W, while the outflow temperature transports were  $-26.0 \pm 3.1 \times 10^{14}$  W (without seamounts) or  $-27.2 \pm 2.3 \times 10^{14}$  W (with rectangular seamounts) through the eastern section, and  $-2.4 \pm 0.2 \times 10^{14}$  W through the northern section. The net horizontal heat flux through the triangle was thus  $-0.8 \pm 3.2$  (without seamounts) or  $-2.0 \pm 2.9$  (with seamounts)  $\times 10^{14}$  W, which equals the estimated net surface heat loss of  $-0.1 \times 10^{14}$  W due to wintertime air-sea interaction within experimental error (KONDO, 1976).

The missed temperature transport due to incomplete coverage of the Okinawa Trough can be estimated roughly by using the missed volume transport estimate for the gap

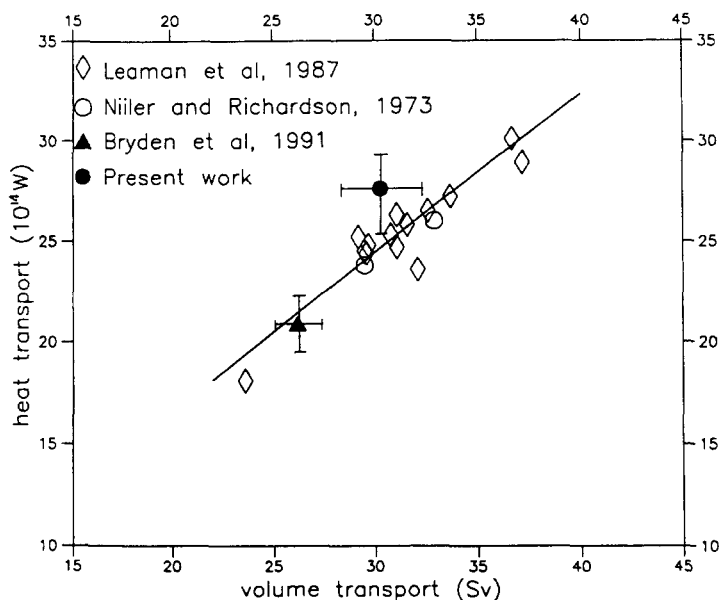


Fig. 2. Summary of temperature and volume transport estimates made in the Kuroshio in the East China Sea (▲, BRYDEN *et al.*, 1991; ●, present work) and in the Florida Current at 27°N (○, NILER and RICHARDSON, 1973; ◇, LEAMAN *et al.*, 1987). Line represents least squares fit of all data

between the southeast corner of the study triangle and the nearest island to the south. If the average potential temperature and density there were 13°C and  $1.028 \times 10^6 \text{ g m}^{-3}$  based on the hydrographic data at Sta. 126, then the missed temperature transport was  $0.7 \times 10^{14} \text{ W}$  for a volume transport of 1.4 Sv, representing only 2.5% of the total temperature transport through the western section. Therefore, our direct estimate of the temperature transport of the Kuroshio through the western section,  $27.6 \pm 1.8 \times 10^{14} \text{ W}$  for a volume transport of  $30.3 \pm 2.0 \text{ Sv}$ , is an accurate estimate of the total Kuroshio temperature transport at 29.5°N in January 1986.

The net annual sea surface heat loss in the Kuroshio southwest of Kyushu has been reported by WYRTKI (1966) and KONDO (1976) to be in the range of  $-50$  to  $-90 \text{ W m}^{-2}$ , with a maximum loss of about  $-350 \text{ W m}^{-2}$  in winter. BUNKER (1980) and ISEMER and HASSE (1987) report similar values for the Florida Current where the net annual sea surface heat loss is about  $-70 \text{ W m}^{-2}$  with a maximum loss of about  $-350 \text{ W m}^{-2}$  in winter. The similarity of air-sea heat fluxes over these two western boundary currents suggests that the Kuroshio and Florida Current may exhibit similar heat flux cycles. The good correlation between temperature transports for the Kuroshio and Florida Current (Fig. 2) implies small variability in potential temperature for the calculation of temperature transport. A linear regression equation fitted to these temperature and volume transports yields a root-mean square deviation of about  $1.1 \times 10^{14} \text{ W}$ , which is generally smaller than the uncertainties in the temperature transport estimates (see LEAMAN *et al.*, 1987), indicating a linear correlation between temperature and volume transports in both the Florida Current and Kuroshio. While additional measurements are required to confirm this relationship for the Kuroshio in the East China Sea, Fig. 2 illustrates a strong similarity

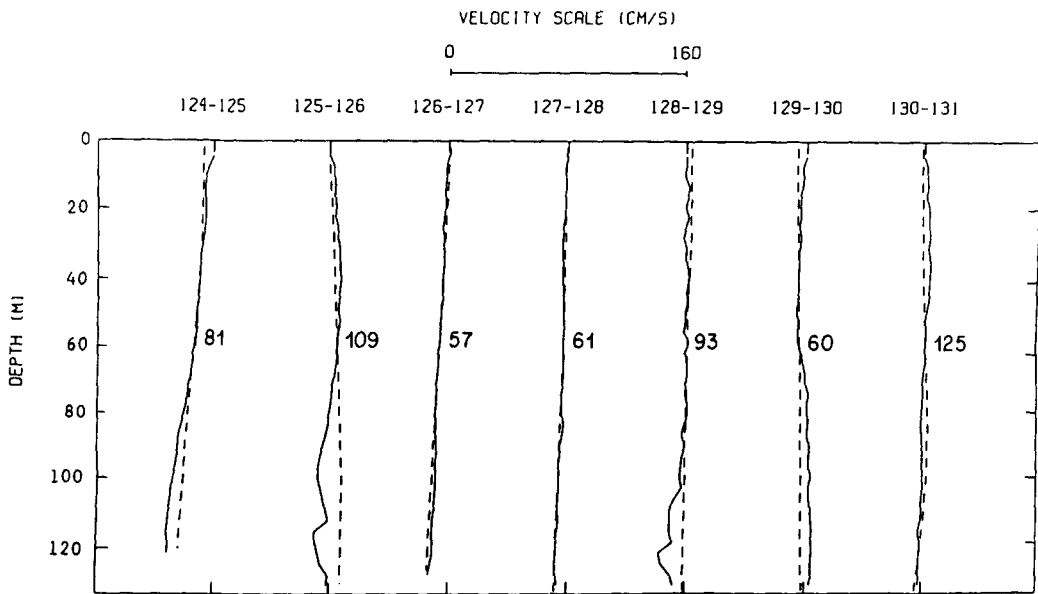


Fig. 3. Some example comparisons between the absolute geostrophic velocity (dashed line) and the averaged ADCP velocity (solid line). The CTD station pair numbers are shown on the top of the figure, and the reference velocity at 60 m for each station pair is indicated in units of  $\text{cm s}^{-1}$ . All comparisons are plotted using the same velocity scale shown at the top of the figure.

between volume and temperature transports in the Kuroshio and Florida Current. One interpretation of the linear relationship exhibited in Fig. 2 is that when the potential temperature across the current is approximately constant, barotropic current fluctuation will cause similar volume and temperature transport variations.

#### 4. STRUCTURE OF THE ABSOLUTE GEOSTROPHIC FLOW FIELD

##### *Test of geostrophic approximation*

In the Kuroshio west of Kyushu, the Rossby number  $R_0 = U/fL$  based on  $f \sim 10^{-4} \text{ s}^{-1}$ ,  $U \sim 1 \text{ m s}^{-1}$  and  $L \sim 10^5 \text{ m}$  is  $\sim 10^{-1}$ , so that the cross-stream momentum balance in the Kuroshio west of Kyushu should be almost geostrophic. Can this basic dynamical balance be demonstrated from our current measurements? The close agreement between vertical shear of absolute geostrophic velocity and the average ADCP velocity profile (Fig. 3) implies that the thermal wind relation is a good approximation in the cross-stream direction in the Kuroshio. The mean difference and deviation between the absolute geostrophic and ADCP velocities averaged over the available depth interval at each station pair throughout the triangle are listed in Table 2: the mean errors are less than  $4.0 \text{ cm s}^{-1}$  in magnitude, and their deviations relative to the mean errors are small except for station pairs 125–126 and 131–132.

At station pair 131–132, the vertical shear of absolute geostrophic velocity was much different from the average ADCP velocity shear, and the deviation relative to the mean exceeded  $7 \text{ cm s}^{-1}$ , an amount greater than 10% of total averaged velocity. This station

pair was located at the northern edge of the Kuroshio outflow and an inflow countercurrent where the radius of curvature  $R$  for the local flow may have been as small as 20 km, yielding a curvature Rossby number  $R_r = U/fR \sim 0.5$ . The observed poor agreement between the geostrophic and ADCP velocity shears was probably due to both curvature and time-dependent effects. The relatively large deviations at station pair 125–126 and several other station pairs may be due to measurement errors in the ADCP since these deviations were all located in the deeper depth bins of the ADCP where the signal-to-noise ratio was relatively small.

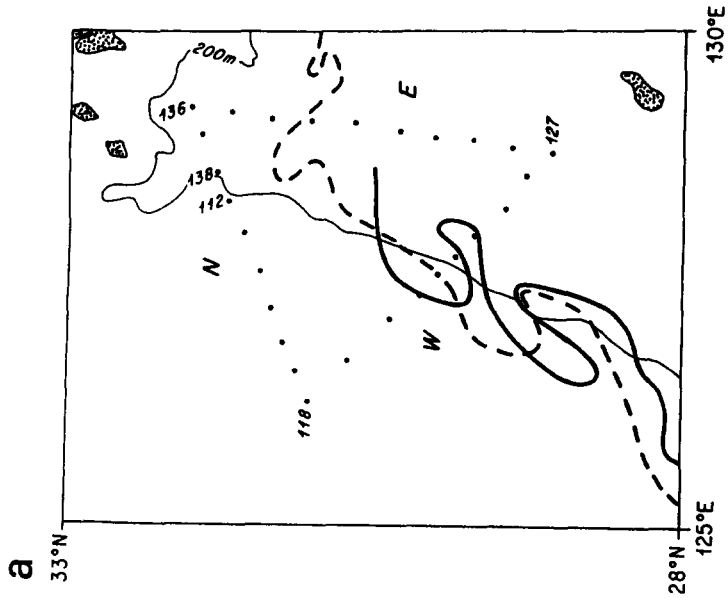
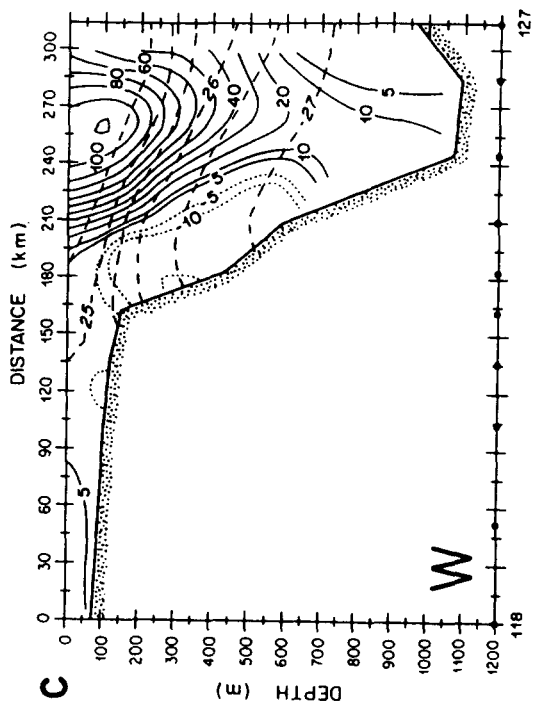
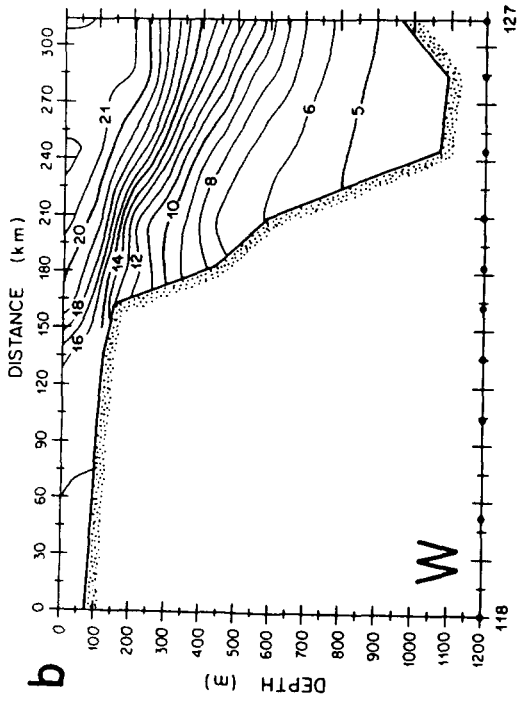
#### *Vertical sections of the absolute geostrophic velocity*

Figure 4 shows the vertical structure of absolute geostrophic velocity across each section of the study triangle. On the western section (Fig. 4c), the maximum velocity of the Kuroshio was found to be about  $110 \text{ cm s}^{-1}$  at a depth of 100 m between Stas 125 and 126. A relatively large vertical velocity shear was located in a range of 200–600 m, corresponding to a large horizontal and vertical gradient of potential density in the main thermocline (see CHEN *et al.*, submitted, for additional discussion of the hydrographic structure). This gradient is indicated by the sloping potential density surfaces in Fig. 4c. A countercurrent of about  $5\text{--}10 \text{ cm s}^{-1}$  was found over the slope and inner shelf, and its maximum velocity was located at a depth of about 300 m. A similar velocity structure also was found over the slope on the northern section (Fig. 4d), suggesting the existence of mesoscale eddies over the slope during the survey. On the eastern section (Fig. 4e), two maximum velocity cores of the Kuroshio were found at a depth of about 100 m on each side

Table 2. Comparison between the averaged ADCP velocity and the absolute geostrophic velocity profiles over the upper water column

Station pair	Mean velocity $\bar{u}$ ( $\text{cm s}^{-1}$ )	Mean difference $\overline{\Delta u}$ ( $\text{cm s}^{-1}$ )	Standard deviation $\sigma_{\Delta u}$ ( $\text{cm s}^{-1}$ )	Depth interval (m)
124–125	78.6	1.7	4.0	4.5–118.5
125–126	125.0	3.2	7.1	4.5–127.5
126–127	57.4	0.4	1.4	4.5–124.5
127–128	59.9	0.3	1.3	4.5–139.5
128–129	89.4	3.6	3.7	4.5–139.5
129–130	63.7	3.5	2.6	4.5–142.5
130–131	123.8	0.5	3.1	4.5–148.5
131–132	53.1	0.5	7.1	4.5–100.5
132–133	53.3	1.2	2.5	4.5–120.5
133.134	15.3	1.9	3.9	4.5–127.5
134–135	19.3	1.1	4.5	4.5–139.5
135–136	32.9	0.1	2.7	4.5–133.5
136–137	27.9	0.3	1.1	4.5–139.5
137–138	5.5	0.7	1.4	4.5–139.5

$\bar{u}$  and  $\overline{\Delta u}$  are the vertical average of the absolute geostrophic velocity and the difference between the absolute geostrophic and ADCP velocities, respectively, computed over the total available depth interval.  $\sigma_{\Delta u}$  is the square root of the vertical average of  $(\Delta u)^2$  computed over the total available depth interval.



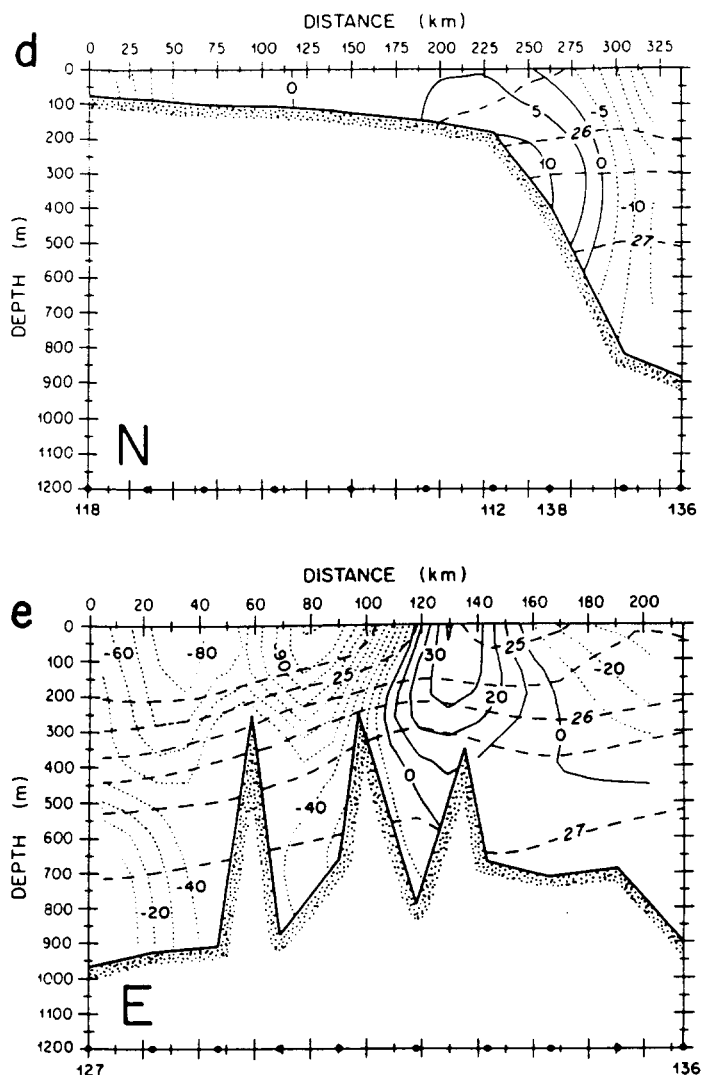


Fig. 4. Sections of absolute geostrophic velocity for the three sides of the study triangle. The CTD station locations and the 200 m isobath are shown in (a), along with the position of the SST front on 28 January (solid line) and 8 February (dashed line) derived from NOAA AVHRR imagery by SUGIMOTO *et al.* (1988). The temperature field on the western (W) sections is shown in (b). The absolute geostrophic velocity on the western (W), northern (N), and eastern (E) sections are shown in (c), (d) and (e), respectively. Velocity convention: inflow is positive, outflow is negative. Contour interval is either 5 or 10  $\text{cm s}^{-1}$ . Also shown on the velocity sections are selected contours of potential density.

of a tall seamount between Stas 128 and 129 and Stas 130 and 131, implying a splitting of the Kuroshio in that region. A countercurrent with a maximum velocity of about  $40 \text{ cm s}^{-1}$  entered the study triangle in the middle of the eastern section between Stas 132 and 133 and flowed out of that region near the northeastern corner of the triangle.

For comparison, we also calculated the geostrophic velocity field relative to the bottom and found that some of the important flow features (e.g. the flow splitting around the seamount on the downstream section and the existence of mesoscale eddies over the slope) were omitted due to the assumption of no motion at the bottom. The actual absolute geostrophic bottom velocity was found to be about  $10 \text{ cm s}^{-1}$  at the center of the Okinawa Trough on the western section, and about  $20\text{--}30 \text{ cm s}^{-1}$  on the eastern section. A bottom velocity of order  $10 \text{ cm s}^{-1}$  also was found by BRYDEN *et al.* (1991) in the upstream region of the Kuroshio near the Ryuku Islands, and by BROOKS and NILLER (1977) in the Florida Strait for the Gulf Stream. It is because of the existence of such bottom velocities in the Kuroshio in the East China Sea that sections of relative geostrophic velocity must be modified by the barotropic part of the absolute velocity. As a result of the large bottom velocities, the maximum velocity of the Kuroshio increased by about  $10 \text{ cm s}^{-1}$  on the western section and by about  $20 \text{ cm s}^{-1}$  on the eastern section. The outflow through the northern section also was increased up to  $20\text{--}30 \text{ cm s}^{-1}$ , and the area of the countercurrent on the eastern section became larger even though its speed did not change appreciably. These results suggest that geostrophic velocity estimates relative to the bottom underestimate the true transport of the Kuroshio in the East China Sea.

#### *Path of the Kuroshio*

The approximate conservation of volume transport through the study triangle allows us to define a transport streamfunction  $\Psi$  by the continuity equation

$$\frac{\partial U}{\partial x} + \frac{\partial V}{\partial y} = 0, \quad (4.1)$$

where  $U = \int_0^h u dz$  and  $V = \int_0^h v dz$  are the volume transports in the water column per horizontal unit. Since

$$V = \frac{\partial \Psi}{\partial x}, \quad (4.2)$$

the streamfunction  $\Psi$  can be found by integrating the above equation with respect to  $x$ , to obtain

$$\Psi(x) = \int_{x_0}^x V dx + \Psi(x_0). \quad (4.3)$$

If  $x_0$  is fixed at the southeastern corner of the triangle, we can set  $\Psi(x_0) = 0$  and use (4.3) to compute  $\Psi$  as a function of  $x$  taken here as the distance along the station sections from  $x_0$ .

The contours of the streamfunction defined by the absolute geostrophic transport (Fig. 5) show clearly the path of the Kuroshio and its adjacent currents in the study area. During the period of the survey, the Kuroshio flowed through the western section as a coherent current and then split into two branches around a seamount as it left through the eastern section. To the north of the Kuroshio, a countercurrent flowed back into the triangle between Stas 131 and 133 on the eastern section. This current went up to the slope first and then turned anticyclonically to leave the study region again near the northeast corner of the triangle. On the western section, a small cyclonic mesoscale eddy was located over the slope, which is consistent with T/S analysis (CHEN *et al.*, submitted). This water property

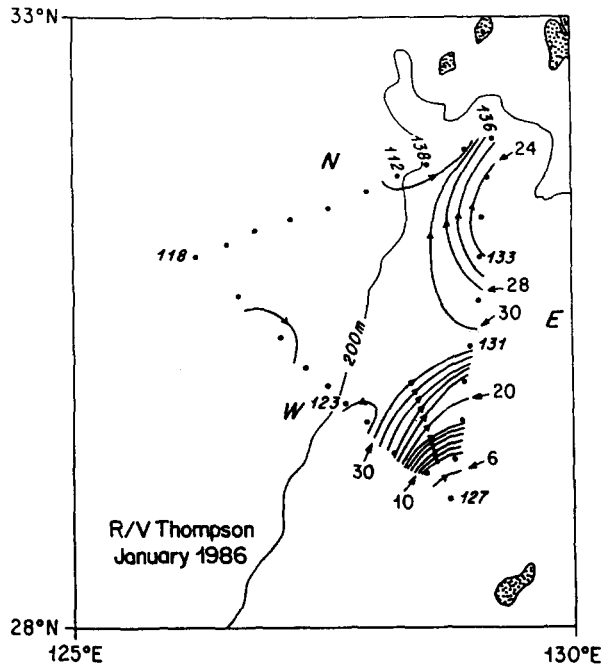


Fig. 5. Streamlines defined by the absolute geostrophic volume transport. Contour interval is  $10^6 \text{ m}^2 \text{ s}^{-1}$ .

analysis also supports the idea that the outflow in the northeast corner of the triangle was drained from both adjacent sides, with most of the outflow being supplied by the anticyclonic eddy.

SUGIMOTO *et al.* (1988) presented a map of the Kuroshio sea surface temperature (SST) front in the East China Sea based on NOAA AVHRR imagery collected on 28 January 1986 (the day the triangular survey started). This map (Fig. 4a) clearly shows the deformation of the Kuroshio SST front over the shelfbreak and upper slope by a cyclonic mesoscale eddy with an approximate radius of 30 km. While the frontal feature is not evident in the surface temperature data collected on the ship (see Fig. 4b), the absolute geostrophic velocity section shown in Fig. 4c nicely illustrates the spatial structure of this eddy. A similar cyclonic eddy feature on the north side of the Kuroshio in this region is seen in the SST image for 3 June 1988 (Fig. 6a). SUGIMOTO *et al.* (1988) also compared the SST frontal position on 28 January 1986 with the subsequent frontal position for 8 February (see Fig. 4a), and while their interpretation is not unique, they did suggest that the eddy was advected downstream by the Kuroshio with a phase speed of order 20–40  $\text{cm s}^{-1}$ . Using a sequence of NOAA AVHRR imagery obtained in Japan for March–April 1986, QIU *et al.* (1990) found that these mesoscale frontal features moved with an average speed of 20–30  $\text{cm s}^{-1}$  and were coherent with Japanese Meteorological Agency moored temperature measurements made at the shelfbreak at 126°20'E, 28°10'N and the north–south sea level tilt across the Tokara Strait. QIU *et al.* (1990) also presented SST imagery and hydrographic data showing the existence of a large anticyclonic warm eddy centered near 31°N, 129°W from mid-May to early June 1986. The warm-core eddy had a radius of

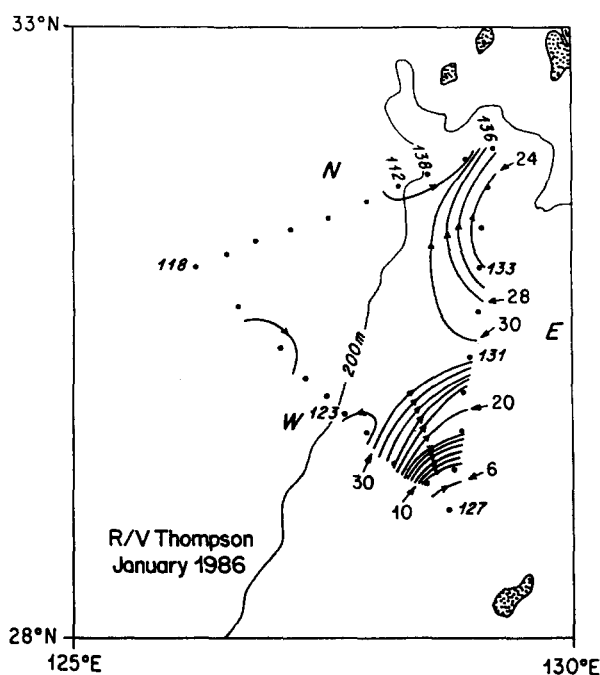


Fig. 5. Streamlines defined by the absolute geostrophic volume transport. Contour interval is  $10^6 \text{ m}^2 \text{ s}^{-1}$ .

analysis also supports the idea that the outflow in the northeast corner of the triangle was drained from both adjacent sides, with most of the outflow being supplied by the anticyclonic eddy.

SUGIMOTO *et al.* (1988) presented a map of the Kuroshio sea surface temperature (SST) front in the East China Sea based on NOAA AVHRR imagery collected on 28 January 1986 (the day the triangular survey started). This map (Fig. 4a) clearly shows the deformation of the Kuroshio SST front over the shelfbreak and upper slope by a cyclonic mesoscale eddy with an approximate radius of 30 km. While the frontal feature is not evident in the surface temperature data collected on the ship (see Fig. 4b), the absolute geostrophic velocity section shown in Fig. 4c nicely illustrates the spatial structure of this eddy. A similar cyclonic eddy feature on the north side of the Kuroshio in this region is seen in the SST image for 3 June 1988 (Fig. 6a). SUGIMOTO *et al.* (1988) also compared the SST frontal position on 28 January 1986 with the subsequent frontal position for 8 February (see Fig. 4a), and while their interpretation is not unique, they did suggest that the eddy was advected downstream by the Kuroshio with a phase speed of order 20–40  $\text{cm s}^{-1}$ . Using a sequence of NOAA AVHRR imagery obtained in Japan for March–April 1986, QIU *et al.* (1990) found that these mesoscale frontal features moved with an average speed of 20–30  $\text{cm s}^{-1}$  and were coherent with Japanese Meteorological Agency moored temperature measurements made at the shelfbreak at  $126^{\circ}20' \text{E}$ ,  $28^{\circ}10' \text{N}$  and the north–south sea level tilt across the Tokara Strait. QIU *et al.* (1990) also presented SST imagery and hydrographic data showing the existence of a large anticyclonic warm eddy centered near  $31^{\circ} \text{N}$ ,  $129^{\circ} \text{W}$  from mid-May to early June 1986. The warm-core eddy had a radius of

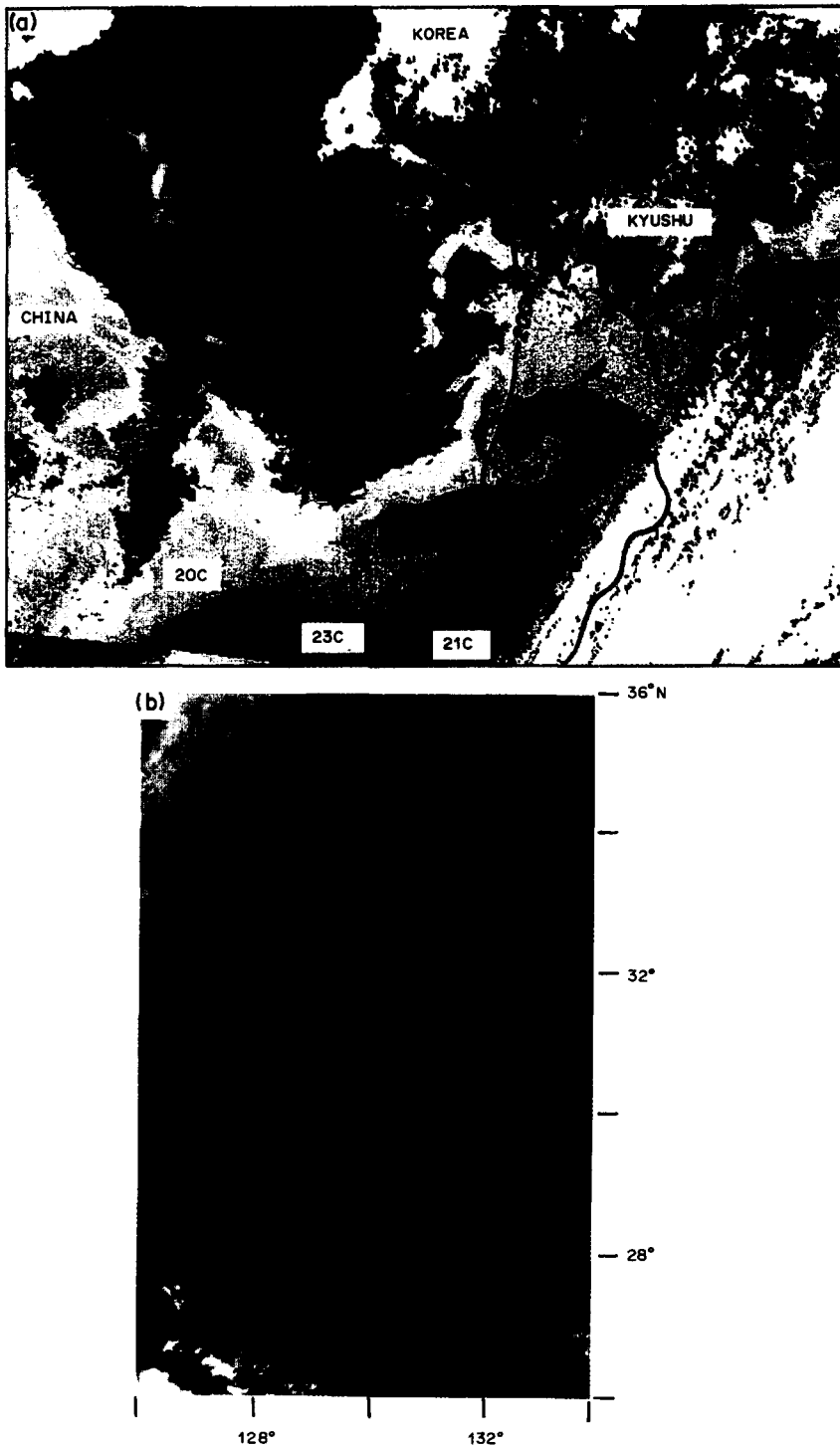


Fig. 6. SST maps for 3 June 1988 (a) and 23 April 1981 (b) derived from NOAA-AVHRR data. Note the presence of mesoscale eddy features along northern edge of the Kuroshio. [These images were kindly supplied by T. Yamagata (a) and G. Lee (b).]



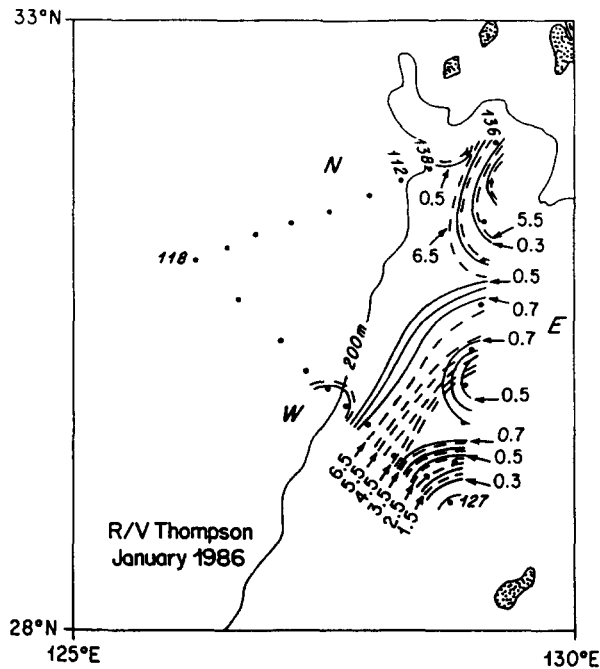


Fig. 8. Plot of the potential vorticity contours (solid line) and streamlines (dashed line) on the potential density surface  $\sigma_\theta = 25.7$ . The units of potential vorticity and the streamline are  $10^{-9} \text{ s}^{-1} \text{ m}^{-1}$  and  $10^4 \text{ m}^2 \text{ s}^{-1}$ , respectively.

those streamlines. However, between the two cores of maximum potential vorticity, Kuroshio water crossed potential vorticity contours as it flowed northeastward and split around the seamount on the eastern section, and potential vorticity (as we have estimated it) was not conserved along the streamlines in that region. To the north of the northern core, potential vorticity contours and streamlines were similar, indicating approximate conservation of potential vorticity on streamlines in that area. Therefore, potential vorticity was conserved along streamlines in the study triangle except between the two cores of maximum potential vorticity where part of the Kuroshio split and flowed through the eastern section on the northern side of the southern seamount.

Since we expect fluid parcels in the central core of the Kuroshio to conserve their potential density and potential vorticity,\* we suggest that the apparent nonconservation of potential vorticity along streamlines near the seamount may be due to the omission of curvature vorticity  $V/R$  in the estimation of potential vorticity using (5.2). If we choose a streamline on the potential density surface  $\sigma_\theta = 25.7$  that starts in the core of maximum

\*In the absence of strong forcing, dissipation and mixing, fluid parcels tend to conserve their potential density and potential vorticity. If the motion is also steady, then parcels will maintain their potential vorticity along streamlines on potential density surfaces. A rough calculation shows that it took about  $1\frac{1}{2}$  days for a parcel to flow from the western section to the eastern section. Since the dominant time scale of variation of the Kuroshio near Kyushu is about 20–40 days (NAGATA and TAKESHITA, 1985), the Kuroshio can be treated as a quasi-steady current during the 2 days we took to sample the study triangle. Moreover, the potential density surface chosen for analysis crossed the maximum potential vorticity regions with large  $\sigma_{\theta z}$  and did not outcrop to the sea surface. As a result, it is unlikely that either surface forcing or convective mixing occurred in such a strongly stratified area.

relative vorticity near the shelf break reduced the total potential vorticity and so there was no longer an abrupt jump in the potential vorticity at the shelf break as found by WATTS (1983), JOHNS (1984) and HALL (1985) for the Gulf Stream. Between the eddy and axis of the Kuroshio, the cyclonic relative vorticity led to an increase of the potential vorticity. To the right of the Kuroshio axis looking downstream, the potential vorticity decreased again due to the anticyclonic relative vorticity. Therefore, a core of maximum potential vorticity with values larger than  $0.7 \times 10^{-9} \text{ s m}^{-1}$  was found in the main thermocline between Stas 123 and 126. This core deepened seaward in the Kuroshio corresponding to the main thermocline structure. In the Kuroshio surface water above the main thermocline, the potential vorticity decreased sharply upward, with values decreasing to  $0.1 \times 10^{-9} \text{ m}^{-1} \text{ s}^{-1}$  or smaller at the surface. In the region deeper than 400 m, the potential vorticity tended toward a uniformly low value with depth, corresponding to the North Pacific Intermediate and Deep Waters.

A similar structure of total potential vorticity was also found on the eastern section near the surface and in the deep regions. Since the Kuroshio split into two branches when it flowed from the western section to the eastern section, the relative vorticity was anticyclonic to the right of each core of maximum velocity (looking downstream), but cyclonic to the left of each core, causing the total potential vorticity to decrease on the right side of the maximum velocity core and increase on the left side. Therefore, two cores of maximum potential vorticity were found to the left sides of the two maximum velocity cores. Since there was a strong countercurrent on the eastern section between Stas 131 and 134, the northern core of potential vorticity covered a relatively larger area than the southern one due to the positive contribution of relative velocity from part of the recirculation.

Two significant similarities can be found between eastern and western sections. First, the three cores of maximum potential vorticity were well-defined and had (within measurement uncertainty) the same maximum value  $>0.7 \times 10^{-9} \text{ s}^{-1} \text{ m}^{-1}$ . Second, looking downstream, the core of maximum potential vorticity was always located to the left of the axis of maximum velocity, thus allowing the path of the Kuroshio to be traced by the core of maximum potential vorticity. This illustrates the importance of including relative vorticity in estimating total potential vorticity, since the distribution of  $f\sigma_z$  showed no evidence of the Kuroshio splitting.

Interestingly, we see no evidence in Fig. 7 of  $18^\circ$  Water (or subtropical mode water in the North Pacific) which is characterized by a minimum potential vorticity. A similar result was shown in the Florida Current by BROOKS and NIELER (1977), who found that the potential vorticity distribution horizontally decreased from the shelf and had a distinct maximum at mid-depth. This suggests that subtropical mode water must have been modified when it left its source region and joined the Kuroshio or it had not yet joined the Kuroshio. WATTS (1983) and JOHNS (1984) indeed showed the trace of  $18^\circ$  Water in the center of the Gulf Stream below the surface water at  $73^\circ$  and  $70^\circ\text{W}$ , where the Gulf Stream had already left the shelf and entered the North Atlantic Ocean. The very strong recirculation observed south of the Gulf Stream in that region implies the intrusion of  $18^\circ$  Water from the interior ocean.

Since the core of maximum potential vorticity split into two cores as the Kuroshio flowed eastward through the study triangle, a semi-enclosed region of relatively low potential vorticity occurred between the two maximum potential vorticity cores on the eastern section (Fig. 8). To the south of the southern core, the contours of potential vorticity were almost parallel to the streamlines, implying that potential vorticity was conserved along

similar to those reported for the Gulf Stream in the Florida Strait, and a roughly linear correlation exists between temperature and volume transports in both regions. As in the Gulf Stream, the structure of potential vorticity in the Kuroshio depends crucially on the distribution of relative vorticity. A comparison of potential vorticity and streamfunction indicates that potential vorticity was conserved along streamlines on potential density surfaces except perhaps near a seamount where curvature vorticity must be considered, and the path of the Kuroshio could be traced by the core of maximum potential vorticity. When looking in the direction of the current, the axis of maximum velocity is located to the right of the core of maximum potential vorticity. Finally, the Kuroshio was potentially unstable as it flowed along the continental margin in the Okinawa Trough because the gradient of potential vorticity on potential density surfaces changed sign across the Kuroshio. This helps explain the mesoscale frontal and eddy features observed in the cyclonic side of the Kuroshio in the East China Sea.

*Acknowledgements*—This research was supported by the National Science Foundation under grants OCE 85-01366, OCE 87-16937 and OCE 87-13988. The CTD and ADCP data were obtained aboard the R.V. *Thompson* with the aid of Chinese and Korean scientists, and we especially thank Kuh Kim and Byung Ho Choi for their help correcting the CTD conductivity data. We also thank Harry Bryden, Dave Chapman, Glenn Flierl, Melinda Hall, Bo Qiu, Paola Rizzoli and John Toole for their helpful comments and suggestions, and Bob Weller and Terry Joyce for their help in understanding the many technical issues involved in obtaining and interpreting ADCP data. Finally, we thank Richard Legeckis, Toshio Yamagata, and Gyung Lee for their help in locating appropriate satellite images to illustrate mesoscale features and producing the complete SST maps shown here in Fig. 6, and an anonymous reviewer who sent us a reprint of SUGIMOTO *et al.* (1988). Anne-Marie Michael took care of the final typing of the manuscript. This is W.H.O.I. contribution no. 7368.

## REFERENCES

- BARTH J. A. and K. H. BRINK (1987) Shipboard acoustic Doppler profiler velocity observations near Point Conception: Spring 1983. *Journal of Geophysical Research*, **92**, 3925–3943.
- BROOKS I. H. and P. P. NIILER (1977) Energetics of the Florida Current. *Journal of Marine Research*, **35**, 163–191.
- BRYDEN H. L., D. H. ROEMMICH and J. A. CHURCH (1991) Ocean heat transport across 24°N in the Pacific. *Deep-Sea Research*, **38**, 297–324.
- BUNKER A. F. (1980) Trends of variables and energy fluxes over the Atlantic Ocean from 1948 to 1972. *Monthly Weather Review*, **108**, 720–732.
- CHAO S. Y. and J. P. MCCREARY (1982) A numerical study of the Kuroshio south of Japan. *Journal of Physical Oceanography*, **12**, 680–693.
- CHEN C. (1989) The structure of the Kuroshio west of Kyushu. M.S. Thesis, MIT/WHOI Joint Program, Woods Hole, MA, 137 pp.
- CHEN C., R. LIMBURGER, R. C. BEARDSLEY and K. KIM (submitted) Comparison of winter and summer hydrographic observations in the Kuroshio and adjacent East China Sea during 1986. *Continental Shelf Research*.
- GROEN P. (1948) Method for estimating dynamic slopes and currents in shallow water. *Journal of Marine Research*, **7**, 313–316.
- HALL M. M. (1985) Horizontal and vertical structure of velocity, potential vorticity and energy in the Gulf Stream. Ph.D. Thesis, MIT/WHOI Joint Program, Woods Hole, MA, 165 pp.
- HALL M. M. and H. BRYDEN (1982) Direct estimates and mechanisms of ocean heat transport. *Deep-Sea Research*, **29**, 339–359.
- ICHIKAWA H. and R. BEARDSLEY (submitted) Temporal and spatial variability of volume transport of the Kuroshio in the East China Sea. *Deep-Sea Research*.
- ISEMER H.-J. and Z. HASSE (1987) *The Bunker climate atlas of the North Atlantic Ocean, volume 2: air-sea interaction*. Springer, Berlin, 252 pp.
- JOHNS W. E. (1984) Geostrophic and potential vorticity in the Gulf Stream northeast of Cape Hatteras. Ph.D. Thesis, University of Rhode Island, Department of Oceanography, Kingston, RI, 232 pp.

potential vorticity on the western section and passes near the seamount on the eastern section, we can simply calculate the value of  $R$  necessary for total potential vorticity to be conserved on that streamline, using

$$q_1 = -\frac{1}{\rho_2} \left( f_2 + \frac{v_2}{R} + \frac{\partial v_2}{\partial n} \right) \frac{\partial \sigma_{\theta 2}}{\partial z}, \quad (5.3)$$

where the subscripts 1 and 2 refer to the values along the streamline on the western and eastern sections, respectively. Based on Figs 2 and 7, with  $q_1 = 0.6 \times 10^{-9} \text{ m}^{-1} \text{ s}^{-1}$ ,  $v_2 = 50 \text{ cm s}^{-1}$ ,  $\partial v_2 / \partial n = -0.27 \times 10^{-4} \text{ s}^{-1}$ ,  $f_2 = 0.6 \times 10^{-4} \text{ s}^{-1}$ , and  $1/\rho_2 \partial \sigma_{\theta 2} / \partial z = -0.1 \times 10^{-4} \text{ m}^{-1}$ , we find that  $R = 18.5 \text{ km}$ . The radius of the seamount between the two maximum potential vorticity cores on the eastern section is about 15 km, the same order as  $R$ . This suggests that curvature vorticity can make an important contribution to the total potential vorticity in regions where the Kuroshio interacts with topographic features like seamounts.

The potential vorticity distribution across the Kuroshio in the western section (Fig. 7) indicates the existence of regions of maximum horizontal and vertical gradients in potential vorticity to the north and south of and above and below the core of maximum potential vorticity on potential density surfaces, respectively. This structure means that the potential vorticity gradient reverses sign on  $\sigma_{\theta}$  surfaces across the Kuroshio or vertical within the Kuroshio, and thus is baroclinically unstable. Below about  $\sigma_{\theta} \sim 27$  (corresponding to water deeper than 600 m), the potential vorticity across the Kuroshio was almost constant, implying that the North Pacific Deep Water was more stable than the main North Pacific Thermocline Water in the Kuroshio. Similar results also were found on the downstream eastern section, where the gradient of potential vorticity changed sign both vertical and across the stream on potential density surfaces. However, because of the complex topography in this region and the splitting of the Kuroshio around one seamount, it is perhaps equally important to consider the influence of bottom topography on the stability of the Kuroshio in this region. Preliminary work by B. Qiu (personal communication) on the dynamic stability of the Kuroshio in the East China Sea indicates that the character of frontal waves on the north wall of the Kuroshio depends critically on the depth of the shelf-break.

## 6. CONCLUSION

The results show that the ADCP velocity shear was in reasonably good agreement with geostrophic shear in the Kuroshio. The Kuroshio entered the study triangle as a coherent current, and then split around a tall seamount into two branches as it left the area. To the north of the Kuroshio, a countercurrent flowed back into the study triangle and then anticyclonically to leave the study region near the northeast corner of the triangle, forming a large anticyclonic eddy west of Kyushu. A small cyclonic mesoscale eddy was found over the slope on the western and northern sections of the study triangle. The core of the Kuroshio was characterized on the western (upstream) section by a maximum surface current of about  $100 \text{ cm s}^{-1}$  and bottom velocities of  $10\text{--}20 \text{ cm s}^{-1}$ , which illustrate the importance of using direct current measurements to reference geostrophic velocity calculations in this region.

The volume transport of the Kuroshio southwest of Kyushu in January 1986 was  $30.3 \pm 2.0 \text{ Sv}$ , and the advective temperature transport was  $27.6 \pm 1.8 \times 10^{14} \text{ W}$ . These values are

## Computations of the geographical distribution of the energy flux to mixing processes via internal tides and the associated vertical circulation in the ocean

BJÖRN SJÖBERG\* and ANDERS STIGEBRANDT†

(Received 24 September 1989; in revised form 22 March 1991; accepted 2 April 1991)

**Abstract**—The global flux of tidal energy to mixing processes via topographically generated internal waves is estimated utilizing gridded databases for bathymetry, vertical density stratification and barotropic tides together with a simple, local model for the generation of progressive internal tides at vertical steps in the ocean floor. Both the horizontal distribution of the energy flux to internal tides and its ocean mean are discussed. The computed oceanic mean value is  $44 \times 10^{-4} \text{ W m}^{-2}$ , a factor of about 2–3 greater than previous estimates (MUNK, 1966, *Deep-Sea Research*, 13, 707–730; BELL, 1975, *Journal of Geophysical Research*, 80, 320–327).

The global distribution of vertical diffusivity in the abyss is computed by assuming that topographically generated baroclinic motions dissipate locally and that the dissipation is distributed vertically according to an empirical law. Our results are linearly dependent on the flux Richardson number  $R_f$ . From the computed vertical diffusivities and the known vertical stratification we finally compute the global distribution of vertical velocities. Choosing a value of  $R_f \approx 0.05$  we obtain an upward vertical transport in the interior of the ocean, at the 1000 m level, of about  $15 \times 10^6 \text{ m}^3 \text{ s}^{-1}$ , which agrees with WARREN's (1981, in: *Evolution of physical oceanography*, B. A. WARREN and C. WUNSCH, editors, 6–41) estimated rate of sinking from surface waters at high latitudes. Below the 1000 m level the upward vertical transport increases and a maximum value of about  $25 \times 10^6 \text{ m}^3 \text{ s}^{-1}$  is found at the 2000 m level, after which the transport decreases to about  $8 \times 10^6 \text{ m}^3 \text{ s}^{-1}$  at the 4000 m level. This may be explained by the action of bottom currents. These currents entrain ambient water whereby the upward interior vertical transports tend to increase with depth. However, because of the entrainment of lighter ambient fluid the dense currents become less dense and only the most dense flows penetrate to the greatest depths.

### 1. INTRODUCTION

MUNK (1966) discussed the vertical circulation of the ocean below the thermocline by use of a stationary one-dimensional model in which vertical advection was assumed to be balanced by vertical diffusion for a conservative tracer. The renewal of bottom water was assumed to take place at great depths, inducing a constant vertical advective velocity  $w$  (thus assuming vertical side walls). Utilizing the vertical diffusion equation in a diagnostic mode, Munk then determined the ratio between the vertical diffusivity  $\kappa$  and  $w$  from observed salinity and temperature profiles in the north Pacific.  $w$  and  $\kappa$  could then be

---

\*SMHI, Oceanographical Laboratory, Box 2212, S-403 14 Göteborg, Sweden.

†Department of Oceanography, University of Göteborg, Box 4038, S-400 40 Göteborg, Sweden.

- JOYCE T. M. (1989) On *in-situ* "calibration of shipboard ADCPs." *Journal of Atmospheric and Oceanic Technology*, **6**, 169–172.
- JOYCE T. M., D. S. BITTERMAN and K. E. PRADA (1982) Shipboard acoustic profiling of upper ocean currents. *Deep-Sea Research*, **29**, 903–913.
- JOYCE, T. M., C. WUNSCH and S. D. PIERCE (1986) Synoptic Gulf Stream velocity profiles through simultaneous inversion of hydrographic and acoustic Doppler data. *Journal of Geophysical Research*, **91**, 7573–7585.
- KONDO J. (1976) Heat balance of the East China Sea during the air mass transformation experiment. *Journal of the Meteorological Society of Japan*, **54**, 382–398.
- KOSRO P. M. (1985) Shipboard acoustic current profiling during the Coastal Ocean Dynamics Experiment. Ph.D Thesis, Scripps Institution of Oceanography, University of California, San Diego, CA, 119 pp.
- LEAMAN K., R. L. MOLINARI and P. S. VERTES (1987) Structure and variability of the Florida Current at 27°N: April 1982–July 1984. *Journal of Physical Oceanography*, **17**, 565–583.
- MONTGOMERY R. (1974) Comments on "Seasonal variability of the Florida current," by Niiler and Richardson. *Journal of Marine Research*, **32**, 533–534.
- NAGATA Y. (1981) Oceanic conditions in the East China Sea. In: *Proceedings of the Japan–China oceanic study symposium on physical oceanography and marine engineering in the East China Sea, October 28–29, 1981*, Shimizu, Japan, pp. 25–41.
- NAGATA Y and K. TAKESHITA (1985) Variations of the sea surface temperature distribution across the Kuroshio in the Tokara Strait. *Journal of the Oceanographic Society of Japan*, **41**, 244–258.
- NILER P. and W. RICHARDSON (1973) Seasonal variability of the Florida current. *Journal of Marine Research*, **31**, 144–167.
- NITANI T. (1972) Beginning of the Kuroshio. In: *Kuroshio*, H. STOMMEL and K. YOSHIDA, editors, University of Washington Press, pp. 129–156.
- QIU B., T. TODA and N. IMASATO (1990) On Kuroshio Front fluctuations in the East China Sea using satellite and *in-situ* observational data. *Journal of Geophysical Research*, **95**, 18,191–18,204.
- REGIER L. (1982) Mesoscale current fields observed with a shipboard profiling acoustic current meter. *Journal of Physical Oceanography*, **12**, 880–886.
- REID J. L. and A. W. MANTYLA (1976) The effect of the geostrophic flow upon coastal sea elevations in the northern north pacific ocean. *Journal of Geophysical Research*, **81**, 3100–3110.
- TAKEMATSU M., K. KAWATATE, W. KOTERAYAMA, T. SUHARA and H. MITSUYASU (1986) Moored instruments observations in the Kuroshio south of Kyushu. *Journal of the Oceanographical Society of Japan*, **42**, 201–211.
- TANAKA S., T. SUGIMURA, T. NISHIMURA, Y. NINOMIYA and Y. HATAKEYAMA (1982) Compilation of the Kuroshio current vector map from NOAA-6/AVHRR data and consideration of oceanic eddies and the short period fluctuation of the Kuroshio. *Journal of the Remote Sensing Society of Japan*, **2**, 11–30 (in Japanese).
- SUGIMOTO T., S. KIMURA and K. MIYAJI (1988) Meander of the Kuroshio Front and current variability in the East China Sea. *Journal of the Oceanographic Society of Japan*, **44**, 125–135.
- WATTS D. R. (1983) Gulf Stream variability. In: *Eddies in marine science*, A. R. ROBINSON, editor, Springer, New York, pp. 114–144.
- WYRTKI K. (1966) *Seasonal variation of heat exchange and surface temperature in the North Pacific Ocean*, Hawaii Institute of Geophysics, University of Hawaii, 80 pp.